Int. J. Electrochem. Sci., 12 **(2017)** 4044 – 4055, doi: 10.20964/2017.05.81

International Journal of ELECTROCHEMICAL SCIENCE
www.electrochemsci.org

The Electrochemical Corrosion Properties of PANI/Coal Composites on Magnesium Alloys

Yan Wang[1,2,*], *Jun Wang*[2,3] *and Xiaofei Zhang*[4]

[1] Research Center for Engineering Technology of Polymeric Composites of Shanxi Province, North University of China, Taiyuan 030051, People's Republic of China
[2] School of Materials Science and Engineering, North University of China, Taiyuan 030051, People's Republic of China
[3] Technology Center, Shanxi Taigang Stainless Steel Co., Ltd., Taiyuan 030003, People's Republic of China
[4] School of Mechanical and Power Engineering, North University of China, Taiyuan 030051, People's Republic of China
[*]E-mail: wangyan224@nuc.edu.cn

Received: 23 January 2017 / *Accepted:* 19 March 2017 / *Published:* 12 April 2017

A study on the corrosion protection properties of PANI/Coal composites is presented. PANI/Coal composites were synthesized by *in situ* polymerization, and coatings containing epoxy and PANI/Coal composites were prepared on the surface of magnesium alloys. The structure, morphology and properties of the samples were characterized using Fourier transformation infrared (FTIR) spectroscopy, scanning electron microscopy (SEM), and electrochemical impedance spectroscopy (EIS). The FT-IR spectra showed that the acid-doped PANI/Coal composites were successfully synthesized, and the SEM images indicated that the samples had nanorod structures. The EIS results revealed that the corrosion current density and corrosion rate of the PANI/Coal composite coatings decreased by 2~3 orders of magnitude compared to the pure magnesium alloy. The impedance of the PANI/Coal composites at low frequencies was enhanced with the increasing coal content. The results indicated that PANI/Coal composites could prominently improve the corrosion protection properties of magnesium alloys. The protective mechanisms of the PANI/Coal composites are also discussed. The excellent anticorrosive properties can expand the applications of magnesium alloys in harsh environments.

Keywords: PANI/Coal composites, Corrosion, EIS, Magnesium Alloy

1. INTRODUCTION

The desirable properties of low density and high specific strength have caused magnesium alloys to be widely applied in automobiles, aerospace components and the computer industry. Unfortunately, magnesium alloys are easily corroded by environmental conditions, which have seriously limited their widespread application in many fields [1-3]. Moreover, the improvement of the anticorrosion properties of magnesium alloys has attracted the attention of material researchers. The corrosion protection techniques for magnesium alloys have focused on surface treatment using physical vapor deposition, plasma oxidation, chemical conversion treatments, electroless plating, and organic coatings [4-8]. The influence of conducting polymers on the anticorrosion of metals has attracted much interest [9-14]. Within the conducting polymer family, PANI has contributed a dominant proportion for applications in electromagnetic, microwave-absorbing and metal protection. Previous papers have reported that organic PANI coatings can prevent metals from corroding in acid, alkaline and saline media. PANI coatings protect metals due to barrier protection, corrosion inhibition, anodic protection, shifting the electrochemical interface, etc. [15-16]. Scientists have improved the functional and processing properties of PANI using inorganic/organic composites and have applied them in the anticorrosion field for metals [19-21]. Abacip [22] showed that the presence of TiO_2 in PANI coatings can improve the anticorrosion properties of A304 steel due to the formation of a coating layer on the metallic surface that behaves like a physical barrier against aggressive medium attack. Kumar [23] studied the effects of polyaniline/f-MWCNT nanocomposites on the protection of steel and indicated that the incorporation of CNTs showed a remarkable improvement in the corrosion resistance. Mostafaei [24] discussed the properties of epoxy/polyaniline-ZnO nanorod hybrid nanocomposite coatings. The results showed that the presence of ZnO nanorods inside PANI can significantly improve the barrier and corrosion protection performance. Zhang [25] prepared epoxy coatings containing polyaniline/organophilic montmorillonite composites and studied the corrosion protection properties on a magnesium alloy. The EIS results indicated that the PANI/OMMT coatings exhibited higher corrosion protective properties compared to contrasting coatings. Zhou [26-27] prepared coal-based polyaniline coatings and studied the anticorrosion behaviors on steel; the experimental results explained that coal could remarkably improve the corrosion resistance of steel.

So far, organic coatings on magnesium alloy surfaces have contained conducting polymers and organic/inorganic composites. The combination and application of PANI and coal for corrosion protection have rarely been reported. The conducting properties of coal are closely connected to their macromolecule structure. Compared to other organic minerals, coal can be used as a template for polyaniline composites. The aromatic layer structures can render the aniline monomers polymerized between their layers. Advanced porous structures can provide numerous channels to produce an interpenetrating network structure. Coal can be used as proton acid to obtain acid-doped PANI.

In this work, PANI/coal powders were synthesized by *in situ* polymerization, and the structures of the composites were characterized. Coatings containing PANI/Coal composites and epoxy as a binder were obtained on a magnesium alloy, and their corrosion resistant properties in NaCl solutions were studied.

2. MATERIALS AND METHODS

2.1 Chemicals and materials

All the chemical reagents, except coal powder, used in this work were of analytical reagent grade and were obtained from different sources. The aniline monomer was distilled, and the coal was ground before use; the other chemical reagents were used without any further purification. Aniline, dodecyl benzenesulfonic acid (DBSA), p-toluene sulfonic acid (TSA), hydrochloric acid (HCl), ammonium peroxydisulfate ($(NH_4)_2S_2O_8$, APS), sodium chloride (NaCl), and diethylenetriamine were purchased from Tianjin Kemiou Chemical Reagent Co., Ltd. (China). The coal powders were provided by Jincheng Anthracite Mining Group. The components of the coal are listed in Tab. 1.

Table 1. Proximate analysis and ultimate analysis of the coal /%

M_{ad}	A_{ad}	V_{ad}	FC_{ad}	S
6	7.41	32.46	60.13	1

2.2 Synthesis of the PANI/Coal composites

The conductive PANI/Coal composites were synthesized in different acids (HCl, DBSA, TSA) by using an *in situ* polymerization method. The detailed process is described as follows. First, a certain amount of the coal particles was suspended in a 0.5 mol/L acid solution and stirred at ambient temperature for 30 min to produce a fine aqueous dispersion. Then, 5 mL of aniline was added into the above solution and then the mixture was stirred in an ice water bath for 30 min. An APS solution of 12.5 g in 0.5 mol/L acids was then slowly added dropwise to the suspension mixture under constant stirring, and the color of the solution in the reactor changed as follows: reddish brown → light yellow → bluish green → dark green. The solutions were allowed to rest without stirring for 24 h. The products were obtained by filtration and washing. Finally, the dark green powders were dried under vacuum at 60 ℃ for 12 h.

2.3 Preparation of the PANI/Coal/epoxy coatings

A certain amount of synthesized PANI/Coal powders was dispersed in an epoxy and diethylenetriamine system using ultrasound. Alcohol and diethylenetriamine were used as the solvent and curing agent, respectively. The magnesium alloy specimens were used for the subsequent corrosion studies, with dimensions of 1×1×3 cm^3. The test surfaces of the metal specimens were mechanically polished using 400 grade and 1000 grade emery paper in turn, followed by a cleaning process with acetone and ethanol, and then dried at room temperature before use. The above

PANI/Coal/epoxy solutions were coated on the test surfaces of the magnesium alloy pillars; the other five planes were encapsulated with adhesive. Then, the samples were cured at room temperature for 24 h.

2.4 Measurements

The FT-IR spectra of the polymer composites were recorded using a Bruker Optics Tensor37 with the KBr pellet technique over the wavenumber range of 400-4000 cm^{-1}. The morphology of the samples was investigated using a Nova NanoSEM 430 with an operating voltage of 20 kV and a working distance of 10 mm. The anticorrosion properties of the samples with and without coatings were tested using Tafel curves and electrochemical impedance spectroscopy (EIS) (RST5202F, current=+/-2.0A). All the measurements were carried out by immersion in a 3.5% NaCl solution at room temperature, with Pt as the counter electrode and a standard calomel electrode as the reference electrode. The corrosion potential (E_{corr}), corrosion current density (I_{corr}) and Tafel slopes were obtained from the Tafel extrapolation method with a scan rate of 0.001 V/s. EIS measurements were carried out at a frequency range of 100 kHz to 0.01 Hz with an amplitude of 5 mV.

3. RESULTS AND DISCUSSION

3.1. FTIR Analysis

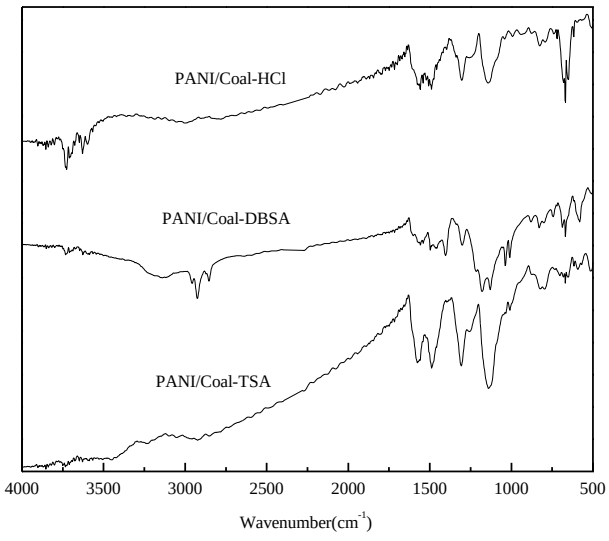

Figure 1. The FT-IR spectra of the PANI/Coal composites doped with different acids

The FTIR spectra of the PANI/Coal composites synthesized with different acids are shown in Fig. 1. It is clearly shown that the FTIR spectra of all samples were very similar. The peaks at 820 cm^{-1} and 1145 cm^{-1} were attributed to the 1,4-bis substituted C-H group bending out of plane in the benzenoid ring and the C-H plane stretching vibration of the N-Q-N quinoid rings. The peak at 1035

cm^{-1} was attributed to S=O stretching bonds. The peak at 1300 cm^{-1} was attributed to the C-N stretching of the benzenoid ring. The peaks at 1573 cm^{-1} and 1489 cm^{-1} were attributed to the C=C stretching of the quinoid rings and benzenoid rings, respectively. The existence of the benzenoid and quinoid units indicated the emeraldine structure of PANI. The peak at 1009 cm^{-1} was attributed to the C-H in-plane bending vibration of the benzenoid with sulfonic acid. Compared to the PANI/Coal composites doped with HCl, there was evidence of peak shifts when the acids were replaced with DBSA and TSA. These shifts consisted of 1145 cm^{-1} to 1134 cm^{-1} and 1130 cm^{-1} and 1573 cm^{-1} to 1566 cm^{-1} and 1565 cm^{-1}. The corresponding characteristic peaks were redshifted to lower wavenumbers. This indicates that the acids were doped into the quinondiimine unit. Introducing the electron withdrawing group SO_3^{2-} decreased the electron density and atomic force constants, causing an inductive effect [1, 25]. The delocalization effect caused by the long chain organic acids decreased the force constants of the quinone rings, causing a conjugation effect. The effects mentioned above decreased the vibration frequency of the bonds. The FTIR results suggest that the acid-doped structure was successfully synthesized.

3.2. SEM Analysis

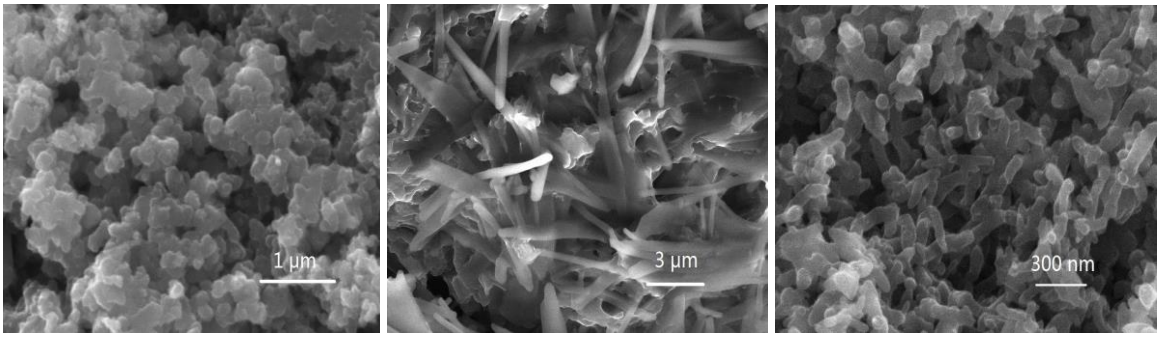

(a) (b) (c)

Figure 2. SEM images of (a) PANI/Coal composites doped with HCl, (b) PANI/Coal composites doped with DBSA, and (c) PANI/Coal composites doped with TSA

PANI/Coal composites with different morphologies were obtained by changing the doping acids. Fig. 2 presents the SEM images of the PANI/Coal powders synthesized in various acid solutions. For all the samples, the coal surfaces were covered by layered PANI composites. It can be seen that the PANI/Coal composites doped with HCl exhibited a sponge structure with irregular agglomerations, and there were also some nanotubes with slick surfaces. When the doped acid was changed to DBSA, the composites revealed a flaky morphology with larger sizes, and their form was not regular. The PANI/Coal composites doped with TSA presented nanofiber and nanorod structures with a smooth surface.

3.3 Tafel Curve Studies

The corrosion protection properties of the magnesium alloy coated with acid-doped PANI/Coal composites were characterized using Tafel polarization curves, as shown in Fig. 3. The corrosion potential (E_{corr}), corrosion current (I_{corr}), corrosion rate (CR) and Tafel slops obtained from the Tafel curves were listed in Tab. 2. The corrosion rate (CR) was calculated using the following equation.

$$CR = I_{corr} \times 3.27 \times 10^3 \times \frac{m}{nd} (mmpy)$$

In this equation, CR is the corrosion rate (mmpy), I_{corr} is the corrosion current density (μA/cm^2), m is the atomic weight of the metal, n is the number of electrons lost during corrosion, and d is the density of the substrate (g/cm^3).

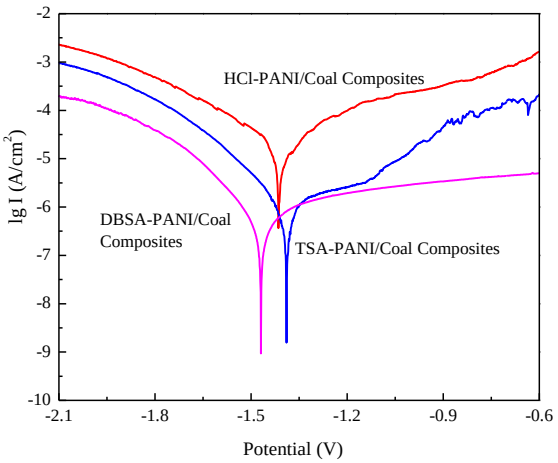

Figure 3. The Tafel curves of the PANI/Coal composites with different doped acids

Table 2. The corrosion potential, corrosion current density and corrosion rate of different acid-doped PANI/Coal composite-coated metal samples in a 3.5% NaCl solution

	E_{corr} (V/SCE)	I_{corr} (μA/cm^2)	Corrosion rate (CR, mm/year)	b_a (mV/dec)	b_c (mV/dec)
Magnesium Alloy	-1.5222	683.91	14.909	510	325
PANI+Coal coatings					
HCl-PANI/Coal composites	-1.4221	31.94	0.696	420	186
TSA-PANI/Coal composites	-1.3861	3.26	0.071	362	138
DBSA-PANI/Coal composites	-1.4667	0.43	0.009	459	88

The magnesium alloys protected with the acid-doped PANI/Coal composite epoxy resin coatings showed lower I_{corr} and CR values than the pure magnesium alloy. In the 3.5% NaCl solution, the corrosive data of the PANI/Coal composite coating were different with various acids. The

corrosion potential (E_{corr}), corrosion current density (I_{corr}) and corrosion rate(CR) of the pure magnesium alloy were found to be -1.5222 V, 683.91 μA/cm^2 and 14.909 mm/year, respectively. When the magnesium alloy substrate was coated with the PANI/Coal composite layer, the corrosion potential shifted in the positive direction, and the corrosion current density and corrosion rate decreased. From Fig. 3 and Tab. 2, it can be seen that E_{corr} increased to -1.4221, -1.3861, and -1.4667 V with the different doped acids. Accordingly, the I_{corr} decreased to 31.94, 3.26 and 0.43 μA/cm^2, corresponding to a reduction of approximately 3~4 decades. The corrosion rate decreased from 0.696 to 0.071 and 0.009 mmpy. The anodic (b_a) and cathodic (b_c) slopes of the Tafel lines were affected by the doped acids, and the anodic slopes were higher than the cathodic slopes, which indicated that the anodic corrosion process of the samples was controlled by the anodic reactions. Then, the Tafel slopes were correlated to the corrosion potential and corrosion current density. This correlation was due to the shielding effect and inactivation and inhibition actions of the PANI and PANI composites, which could improve the corrosion inhibitive effect of the composite coatings and thus enhance the magnesium alloy's resistance to corrosion. The anticorrosion mechanism of the PANI coating originated from the formation of the protective layer, which was developed from the redox reaction of the acid-doped PANI. During the oxidation-reduction reaction of PANI, the released anions of the acid reacted with metal cations and produced insoluble or complex compounds that could protect the magnesium alloy coupons. When the PANI was prepared in the DBSA and TSA environment, the larger molecular sizes of the doped acids also ensured greater adsorption on the surfaces of the magnesium alloy samples and decreased the effective area for the corrosion reaction by blocking the reaction sites [32]. It was demonstrated by some papers that acids doped PANI could improve the corrosion protective property of magnesium alloy [1, 25, 33]. Rajasekharan [28] claimed the aliphatic organic acid doped polyaniline coatings could significantly improve the anticorrosion performance of the steel.

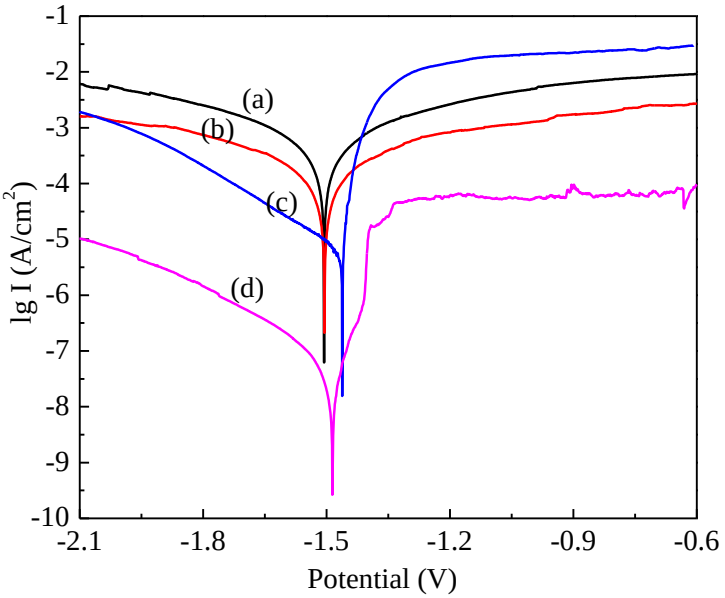

Figure 4. The Tafel curves of the pure magnesium alloy (a), PANI-Epoxy coating (b), PANI/30% Coal-Epoxy coating (c), and PANI/70% Coal-Epoxy coating (d).

Table 3. The corrosion potential, corrosion current density and corrosion rate of the pure magnesium alloy, PANI-Epoxy coating, PANI/30% Coal-Epoxy coating and PANI/70% Coal-Epoxy coating

	E_{corr}（V/SCE）	I_{corr} (μA/cm^2)	Corrosion rate (CR, mm/year)	b_a (mV/dec)	b_c (mV/dec)
Magnesium Alloy	-1.5222	683.91	14.909	510	325
PANI-Epoxy coating	-1.5181	111.378	2.428	293	241
PANI/30% Coal-Epoxy coating	-1.4570	9.840	0.215	180	161
PANI/70% Coal-Epoxy coating	-1.4937	0.0683	0.001	65	139

Coal has a unique porous and aromatic ring structure; the numerous functional groups in coal are mainly phenolic hydroxyl, carboxyl and ether bonds. Hence, comprehensive investigations of coal have attracted the attention of researchers. Herein, composites of coal and PANI were synthesized, which were added into epoxy coatings as functional fillers. The anticorrosion properties of the above coatings on the magnesium alloy blocks were also studied. The Tafel curves of the pure magnesium alloy, PANI coating, and PANI/Coal composite coating are exhibited in Fig. 4. The data derived from the Tafel curves are given in Tab. 3. The results in the figure and table show that the introduction of coal significantly improved the anticorrosion properties. The corrosion potential shifted from -1.5222 to -1.4570 mV/SCE, changing by 65 mV/SCE. The corrosion current density and corrosion rate of the PANI/Coal composite coatings decreased significantly. When the added levels of coal reached 30% and 70%, the I_{corr} values reduced from 683.91 and 111.378 μA/cm^2 to 9.840 and 0.0683μA /cm^2, respectively. The I_{corr} reduction due to the PANI/Coal composites was approximately 2~4 orders compared to those of the magnesium alloy and PANI coating. The CR changed from 14.909 and 2.428 mm/year to 0.215 and 0.001 mm/year, respectively. The slopes of the polarization curves of the PANI/Coal composites coatings were lower than those of the pure magnesium alloy and PANI-Epoxy coating, and their effects on the Tafel slopes were similar to those of the other parameters. Undoubtedly, the PANI/Coal composite coatings exhibited excellent corrosion protective behaviors. The pores and active functional groups of the PNAI/Coal composites could react with the epoxy matrix and produce a crosslinked structure that improved the shielding effect of the coating. The other active functional groups and pores captured the corrosive ions that penetrated into the coating. The capturing effect caused the corrosive ions to remain in the pores or prolong the permeation time of the ions. All of the above mechanisms could reduce the number of ions that penetrated into the coating and delay the process of corrosive ions on the metal surface, which increased the anticorrosion properties of the coatings [26].

3.4 Corrosion Protection Performance of the PANI/Coal Composite-Coated Magnesium Alloy

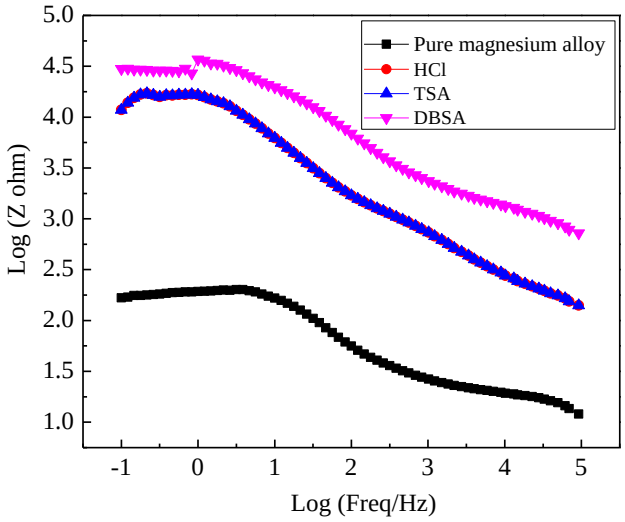

Figure 5. The EIS curves of the pure magnesium alloy and PANI/Coal composite coatings with different acids

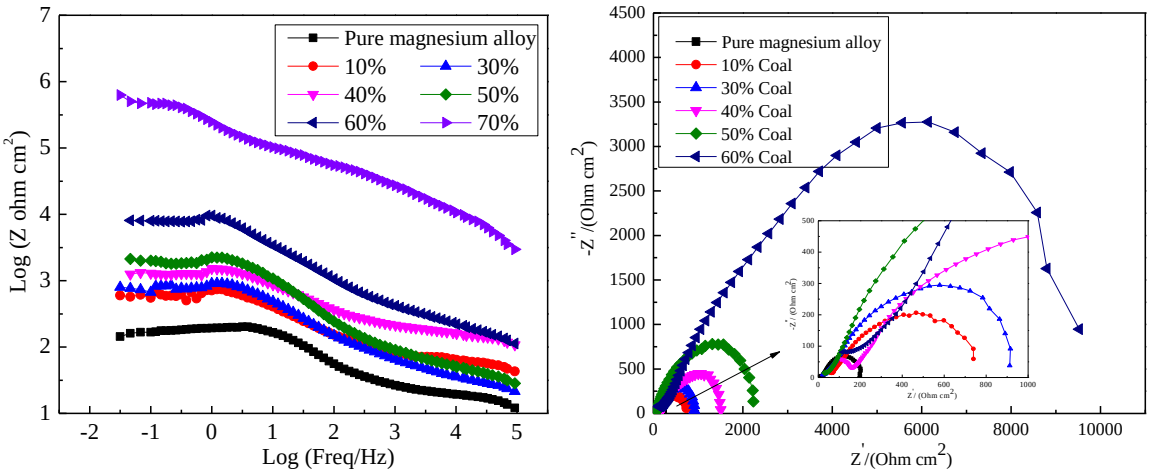

(a) (b)

Figure 6. Bode plots (a) and Nyquist curves (b) of the PANI/Coal composite coatings with different coal contents

Magnesium can react with oxygen and form oxide film products, but the films exhibit poor protection capabilities for magnesium alloys due to their loose structure. The applications of magnesium alloys are thus seriously limited, and improving the anticorrosion properties of magnesium alloys has important practical significance. In this study, EIS tests were conducted to characterize the anticorrosion ability of PANI coatings on magnesium alloys. Fig. 5 shows the Bode impedance curves for the pure and acid-doped PANI/Coal composite coatings in 3.5% NaCl solutions. The plots indicate that the impedances of the acid-doped PANI composites were much higher than those of the uncoated metal. The impedance values of the HCl-doped and TSA-doped samples were very close to each other,

and they were both lower than that of the DBSA-doped PANI/Coal composite coating. The results show that the acid-doped PANI/Coal composites could improve the corrosion protection properties of the magnesium alloy. Compared to an inorganic acid, such as HCl, larger molecule organic acids contained some functional groups that could protect the materials from corrosion.

Magnesium alloys have numerous desirable properties, such as low density, high specific strength, and excellent machinability. However, their poor anticorrosion properties have limited their applications. The coatings of PANI/Coal composites were used for protecting magnesium alloys. Electrochemical impedance spectroscopy is an important method that can provide valuable data on the capacitor behavior of modified electrodes. To date, EIS has been applied widely to investigate the corrosion resistance behavior of different polymers as protective coatings against corrosion. EIS curves for PANI coatings with different coal contents are presented in the Bode plots and Nyquist diagrams shown in Fig. 6. It can be seen that the EIS curves of all the samples exhibited similar trends. The impedance spectra [3] at low frequencies could be used to express the total corrosion resistance conferred by the coatings. The results in Fig. 6(a) indicated that the impedance of the composite coatings at 0.1 Hz increased with the enhancement of the coal content, and the alloys with the coatings exhibited a markedly higher impedance value compared to the pure magnesium alloy. At first, there was a difference of approximately four orders of magnitude between the impedance data among all the samples. Then, the PANI/70% coal system showed relatively better barrier properties at low frequencies with 10^5-10^6 Ωcm^2, whereas the |Z| at 0.1 Hz was found to be near 10^3-10^4 Ωcm^2 for the other PANI/Coal systems. All of these values were much higher than that of the pure magnesium alloy with 10^2 Ωcm^2 at 0.1 Hz. Displayed in the Nyquist plots in Fig. 6 (b), increased semicircles were obtained with the increasing coal content. For the uncoated magnesium alloy, the EIS diagram reflected the formation of a corrosion film on the metal surface. For the coated samples, the PANI/Coal composite coatings had certain corrosion resistance abilities, but the poorer barrier properties of the lower coal content samples led to a low resistance. With the increasing additive coal content, the passive and barrier effects of the coatings produced several increased semicircles.

There were several possible mechanisms for explaining the protection properties of the PANI coatings, including shielding effects, barrier protection, anodic protection, corrosion inhibition, and the formation of an insoluble counter-anion salt [1]. The most important effect of the PANI coatings was the shielding effect from corrosive ions. The numerous void structures and functional groups in the coal could react with the epoxy matrix, and they formed a crosslinked interpenetrating network. This crosslinked structure improved the shielding effects of the coating. The diffusion process of the electrolyte into the metal surface through the PANI/Coal coatings was more difficult than that of the other systems. The excellent shielding and barrier properties of the PANI/Coal coatings could hinder the penetration of aggressive ions, and improve the anticorrosion properties of the magnesium alloy. The functional groups and pore structure could capture the corrosive ions, which made the ions remain in the pores for longer times or delayed the time of penetration to the substrate surface. All of these effects improved the corrosion resistance properties by reducing the numbers of corrosive ions or prolonging the diffusion process of the ions to the metal surface. Similar results have been shown that the combination of carbon based additives and PANI reinforced the anticorrosive performance of coatings, and the improvement effect was enhanced by the increasing of carbon additives [29~31].

Generally, the anticorrosion ability of the PANI/Coal composite coatings could be attributed to the passivating effect due to the oxidation of its emeraldine state. PANI can be reconverted between an emeraldine state (EB) and leuco base state (LB) by an oxidation-reduction reaction, such as the following equation [32].

$$Mg \longrightarrow Mg^{2+} + 2e$$

$$PANI(EB) \underset{+e^-}{\overset{-e^-}{\rightleftharpoons}} PANI(LB)$$

$$2H_2O+O_2+2e^- \longrightarrow 4OH^-$$

The redox process can produce a passive film that exists between the PANI/Coal coating and metal surface. During the cyclic process, the coating could provide higher corrosion protection for the magnesium alloy [33, 34]. On the other hand, PANI/Coal could transfer the charges. The charges required for the cathodic reaction could be delivered to the interface between the electrolyte and the PANI/Coal composites across the coatings. This process could prevent the cathodic reaction at coating/metal interface, which would avoid the metal corrosion and adhesion invalidation of the coating. During the electrochemical process, the surplus charges of the magnesium alloy could be transferred from the interface between the metal and coating to the interface between the coating and electrolyte, which could enrich the positive charges at interface between the metal and coating and increase the anodic polarization, achieving anodic protection. In summary, all of the mechanisms above provided a better corrosion protection effect in the PANI/Coal composite coatings [26-27].

4. CONCLUSIONS

PANI/Coal powders were synthesized by *in situ* polymerization. Coatings based on epoxy and PANI/Coal composites were prepared on the surfaces of magnesium alloys. The FTIR spectra showed that acid-doped PANI/Coal composites were successfully synthesized. The Tafel curves in a 3.5% NaCl solution revealed that the corrosion current density and corrosion rate of the PANI/Coal composite coatings decreased significantly. The impedances of the PANI/Coal composites were enhanced with the increasing coal content. The results indicated that PANI/Coal composites could prominently improve the corrosion protection properties of magnesium alloys. The improvement of the corrosion resistance was mainly due to the shielding effect and anodic protection of the coatings.

ACKNOWLEDGEMENTS
The authors are grateful for the support of the National Natural Science Foundation of China under grant (11202006) and the Shanxi Provincial Natural Science Foundation of China (2014021018-6).

References

1. Y. J. Zhang, Y. W. Shao and T. Zhang, *Corros Sci*., 53(2011) 3747.
2. X. M. Chen, G. Y. Li and J. S. Lian, *T. Nonferr. Metal. Soc.,* 20(2010) s643.
3. S. A. Salman, R. Ichino and M. Okido, *T. Nonferr. Metal. Soc.,* 19(2009) 883.
4. J. J. Fang, K. Xu and L. H. Zhu, *Corros Sci*., 49(2007)4232.
5. T. Lei, C. Ouyang and W. Tang, *Surf. Coat. Technol.,* 204(2010) 3798.

6. A. Hikmet, and S. Hakan, *Mater. Charact*., 59(2008) 266.
7. M. C. Zhao, M. Liu and G. L. Song, *Corros Sci*., 50(2008) 3168.
8. M. Shabani-Nooshabadi, S. M. Ghoreishi and M. Behpour, *Corros Sci*., 53(2011)3035.
9. C. B. Hu, Y. S. Zheng, Y. Q. Qing, F. L. Wang, C. Y. Mo and Q. Mo, *J. Inorg. Organomet. Polm.* Mater. 25(2015) 583.
10. L. G. Ecco, M. Fedel, A. Ahniyaz and F. Deflorian, *Prog. Org. Coat*., 77(2014) 2031.
11. Q. J. Yu, J. Liu, J. M. Xu, Y. Q. Yin, Y. Y. Han and B. X. Li, *J. Sol-Gel Sci. Technol*., 75(2015)74.
12. D. E. Tallman, G. Spinks, A. Dominis and G. G. Wallace, *J. Solid State Electrochem*., 6(2002)73.
13. P. A. Kilmartin, L. Trie and G. A. Wright, *Synth. Met.*, 131(2002) 99.
14. R. C. Rathod, S. S. Umare, V. K. Didolkar, B. H. Shambharkar and A. P. Patil, *T. Indian. I. Metals*., 66(2013) 97.
15. M. Ionit and A. Pruna, *Prog. Org. Coat*., 72(2011) 647.
16. M. Ates and E.Topkaya, *Prog. Org. Coat*., 82(2015) 33.
17. J. Li, H. Q. Xie and Y. Li, *J. Solid State Electrochem*., 16(2012) 795.
18. Y. H. Yu, Y. Y. Lin, C. H. Lin, C. C. Chan and Y. C. Huang, *Polym. Chem*., 5(2014)535.
19. J. Ryu and C. B. Park, *Angew. Chem., Int. Ed*. 48(2009) 4820.
20. P. Piromruen, S. Kongparakul and P. Prasassarakich, *Prog. Org. Coat*., 77(2014) 691.
21. A. Olad and H. Rasouli, *J. Appl. Polym. Sci*., 15(2010) 2221.
22. S. Abaci and B. Nessark, *J. Coat. Technol. Res*., 12(2015)107.
23. A. Madhan Kumar and Z. M. Gasem, *Prog. Org. Coat*., 78(2015) 387.
24. A. Mostafaei and F. Nasirpouri, *Prog. Org. Coat*., 77(2014) 146.
25. Y. J. Zhang, Y. W. Shao, T. Zhang, G. Z. Meng and F. H. Wang, *Prog. Org. Coat*., 76(2013) 804.
26. Y. Q. Deng, L. M. Ge and A. N. Zhou, *Corros & Protect*., 25(2004) 323.
27. Y. Q. Deng, L. M. Ge and A. N. Zhou, *J. Mater. Protect*., 38(2005)11.
28. V. Rajasekharan, T. Stalin, S. Viswanathan and P. Manisankar, *Int. J. Electrochem. Sci.*, 8(2013) 11327.
29. P. P. Deshpande, S. S. Vathare, S. T. Vagge, E. Tomsik and J. Stejskal, *Chem. Pap.*, 67(2013)1072.
30. A. A. Hermas, M. A. Salam and S. S. Al-Juaid, *Prog. Org. Coat*., 76(2013)1810.
31. K. Cai, S. Zuo, S. Luo, C. Yao, W. J. Liu, J. F. Ma, H. H. Mao and Z. Y. L, *RSC Adv.*, 6(2016)95965.
32. A. B. Samui, A. S. Patankar and J. Rangarajan, *Prog. Org. Coat*., 47(2003)1.
33. Y. J. Zhang, Y. W. Shao, G. Z. Meng, T. Zhang, P. Li and F. H. Wang, *J. Coat. Technol. Res*., 12(2015) 777.
34. E. Armelin, C. Alemán and J. I. Iribarren, *Prog. Org. Coat*., 65(2009) 88.